# 4
# UWB Antenna with Band Notch Characteristics

The application of UWB technology for indoor wireless communication is promising and encourages the researchers from academia and industry due to its several advantages. However, it offers challenge among UWB antenna designers due to its detrimental interference issues with other existing systems and services. It is desirable in wireless communications to achieve band rejection characteristics from the existing narrowband interfering systems. The wide spectrum range of UWB technology (3.1-10.6 GHz) includes many other interfering technologies, which operates in the UWB spectrum and causes undue interferences. Hence, UWB antenna should have band rejection characteristics in the possible interfering bands. The objective of this chapter is to design and investigate miniaturized and compact UWB antennas with band notch characteristics. In order to achieve band notch characteristics, fractal and C-shaped slots are introduced in the proposed design and their characteristics are investigated.

## 4.1 Introduction

The UWB system attracts great interest of research community because of its many benefits such as high data rate, low spectral density, low power consumption, etc. However, UWB antenna design faces some interference challenges with some existing narrowband systems such as 3.3-3.69 GHz WiMAX (IEEE 802.16), and 5.15–5.825 GHz WLAN (IEEE 802.11a). Hence, design of an UWB antenna with dual band notch characteristics is very challenging task. The band rejection in above undesired bands can be obtained by introducing slots either in the monopole or in the ground plane of antenna. So far, different notch band UWB antennas are reported in the literature [Gao *et al.*, 2013; Chu and Yang, 2008; Abdollahvand *et al.*, 2010; Ojaroudi and Ojaroudi, 2013; Azim *et al.*, 2014; Cho *et al.*, 2006]. Fractal geometry based slots are etched from the monopole of the antenna to achieve the band rejection [Karmakar *et al.*, 2008; Song *et al.*, 2010]. The analysis and design of these antennas are difficult because of their large structure and complex structure. Thus, design of compact UWB antenna with dual band notch characteristics is required.

## 4.2 Octagonal Shaped UWB Antenna with Dual 3.5/5.5 GHz Band-notched Characteristics

### 4.2.1 Antenna Design

#### (a) Antenna Configuration

In this section, a novel octagonal shaped UWB antenna with dual band notch characteristics is presented. The geometry of the proposed UWB antenna is shown in Figure 4.1. In this design, a fractal notch generated using Minkowski geometry, is etched from the monopole to provide band notch characteristics at 3.5 GHz. The notch at 5.5 GHz is achieved by introducing a pair of C-shaped single split ring resonator (SSRR) on both sides of feed line.

The basic monopole of the antenna is octagonal shape, which provides additional impedance tapering property with feed line. The FR4 substrate of dielectric constant $\varepsilon_r$ = 4.4,

loss tangent tanδ = 0.023 and thickness 1.6 mm is used for antenna design. The simulations of the antenna design are carried out using Ansoft High Frequency Structure Simulator (HFSS v.13). The proposed antenna is fed by a 50 Ω microstrip line. The evolution of the antenna structure is shown in Figure 4.2. The voltage standing wave ratio (VSWR) characteristics for various antennas illustrated in Figure 4.2 is demonstrated in Figure 4.3. In order to obtain the wideband bandwidth, the ground plane is positioned at a distance from the monopole, because the surface current density exists more on the circumference of the monopole and the ground near to monopole. The separation between them affects the impedance matching and return loss characteristic significantly. The introduction of rectangular notch in the ground plane, as shown in Figure 4.2(b), improves the VSWR response at higher frequencies in the UWB operating range. Moreover, the introduction of notch in the structure causes for variation in inductance and capacitance of input impedance. Thus, the improvement in bandwidth is observed due to the generation of additional resonances at higher frequencies.

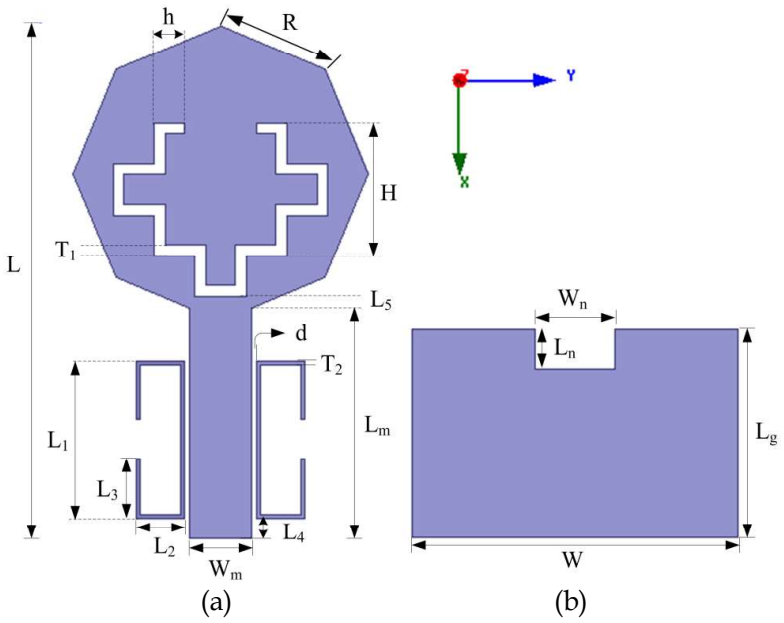


**Figure 4.1:** Geometry of the proposed UWB antenna (a) Radiator portion (b) Ground portion

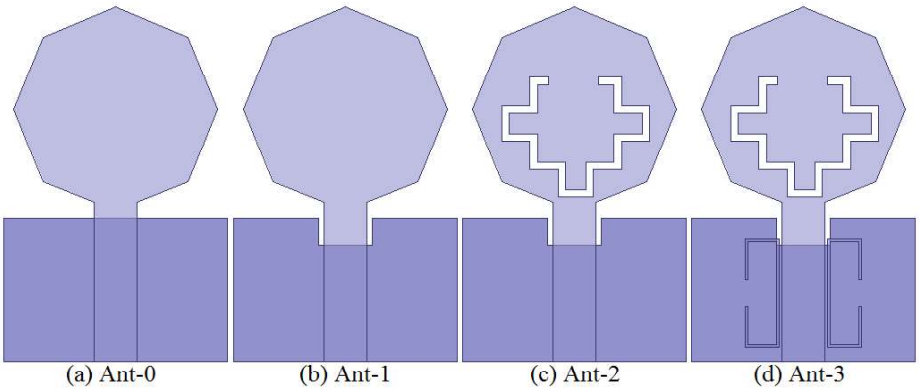


**Figure 4.2:** Evolution of the UWB antenna (a) The initial octagonal shaped antenna, (b) The antenna with rectangular notch in ground plane (c) The antenna with fractal Minkowski and (d) The antenna with fractal notch and dual C-shaped notch

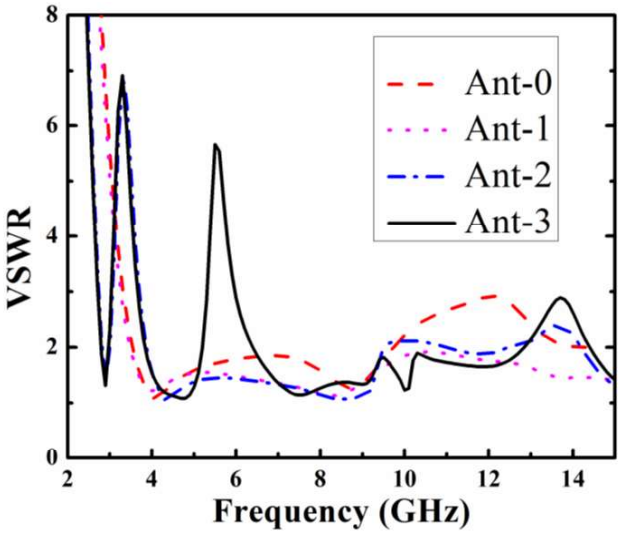


**Figure 4.3:** Simulated VSWR characteristics of the different antenna structure generated in the evolution

**(b) Dual band-notch Characteristics**

In order to achieve the notch band characteristics at WiMAX band, fractal notch is generated using Minkowski fractal geometry and is etched from the monopole of the antenna as shown in Figure 4.2(c). The generation of Minkowski fractal is shown in Figure 4.4. The band rejection at WLAN band is achieved by creating a pair of C-shaped SSRR on both sides of feed line as shown in Figure 4.2(d). Moreover, these structures are placed near to feed line that facilitates strong coupling between them. These modifications in the geometry captures and stores most of the energy and provides filtering characteristics at WiMAX/WLAN bands.

The effective length of the notch is calculated using mathematical equations as [Karmakar *et al.*, 2008; Tripathi *et al.*, 2014]:

$$L = \frac{c}{2f_{notch}\sqrt{\varepsilon_{eff}}} \tag{4.1}$$

$$L_{n1} = 3K + 2h \tag{4.2}$$

$$K = \left(\frac{5}{3}\right)^{n} H \tag{4.3}$$

$$L_{n2} = L_1 + 2L_2 + 2L_3 \tag{4.4}$$

where, c is the speed of light, $\varepsilon_{eff}$ is the effective dielectric constant of the substrate as calculated in [Pozar, 1998], L is desired notch length, $L_{n1}$ and $L_{n2}$ denotes the notch length introduced in the antenna structure, K is the effective length of a single Minkowski fractal section, n is the number of higher order iteration, $f_{notch}$ is centre notch frequency, $\lambda_g$ is the guided wavelength at the desired notch frequency, whereas H, h, $L_1$, $L_2$ and $L_3$ are design parameters. However, the effective length of a single Minkowski fractal segment, K is calculated for a specified value of H and iteration order n using Eq. (4.2).

The fractal shaped notch length is calculated using Eq. (4.2) and (4.3). The length of the second notch band (WLAN) is calculated using Eq. (4.4). These modifications in the geometry provide a wider operational bandwidth and help to achieve the desired UWB characteristics with dual band notch characteristics. Thus, considering such geometrical variations the optimized geometry of the proposed UWB antenna is shown in Figure 3(b). The values of the optimized design parameters are given in Table 4.1.

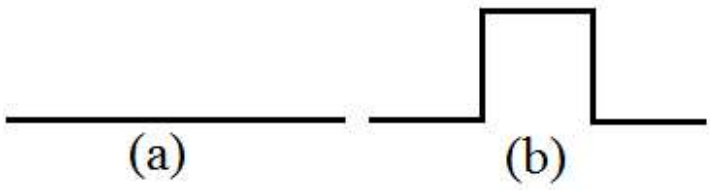


**Figure 4.4:** Recursive generation of Minkowski fractal structure (a) Initial Structure and (b) After first iteration

**Table 4.1:** Optimized geometrical parameters of the proposed UWB antenna

| Parameters | Dimensions (mm) | Parameters | Dimensions (mm) |
|---|---|---|---|
| L | 26.0 | H | 6.5 |
| W | 16.5 | h | 1.5 |
| R | 5.75 | $L_1$ | 8.0 |
| $W_m$ | 3.2 | $L_2$ | 2.5 |
| $L_m$ | 11.6 | $L_3$ | 3.0 |
| $W_n$ | 2.0 | $L_4$ | 1.0 |
| $L_n$ | 4.0 | $L_5$ | 0.35 |
| $L_g$ | 10.5 | $T_1$ | 0.55 |
| d | 0.2 | $T_2$ | 0.2 |

The current distribution pattern of the proposed UWB antenna at 3.5 GHz and 5.5 GHz notch frequencies is shown in Figure 4.5. At 3.5 GHz, the current density is mainly distributed along the edges of fractal structure, whereas at 5.5 GHz it is around C-shaped SSRR near feed line. The direction of current at inner and outer edges of the notch are opposite in directions, so the radiation field generated by each other is cancelled out. This leads to good rejection in those bands. It means at notch bands antenna characteristics are suppressed significantly and structure cannot radiate.

The VSWR variation for different values of H is shown in Figure 4.6. It is observed that notch response and operating bandwidth depends significantly on the value of H. As the value of H increases, notch frequency bands move towards lower frequency. However, at H = 7.5 mm, higher VSWR is observed, whereas for higher frequencies VSWR gets distorted in the UWB band. Figure 4.7 displays the VSWR variation with length $L_1$ from 7.0 mm to 9.0 mm. By increasing $L_1$, the notch band is shifted towards lower frequency, whereas at 7.0 mm and 9.0 mm higher frequency response is distorted. The variation in length of H and $L_1$ changes the resonating length of notch structure as well as affect the coupling between the radiating elements and filter elements, which leads to variation in operational bandwidth and VSWR. Moreover, the variation in one notch band parameter did not affect the other notch response, which means these notch response are independent of each other.

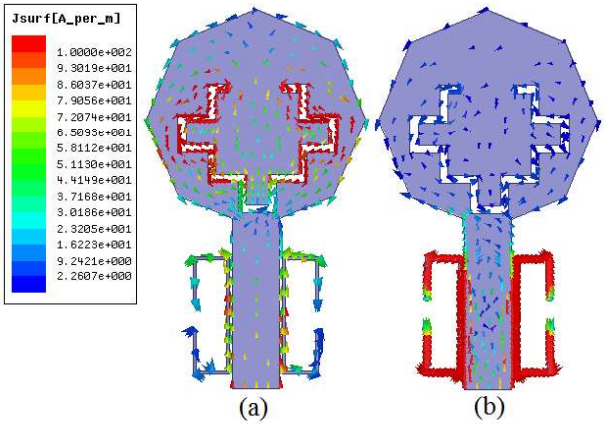


**Figure 4.5:** Simulated surface current distribution in geometry at notch frequency (a) 3.5 GHz and (b) 5.5 GHz

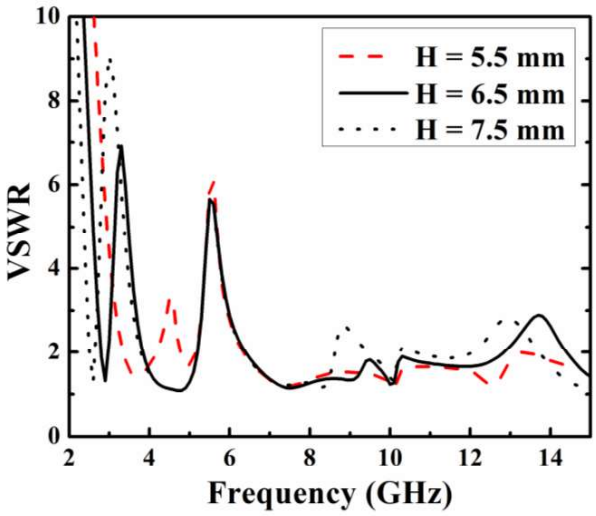


**Figure 4.6:** Simulated VSWR value of the antenna for variation in H

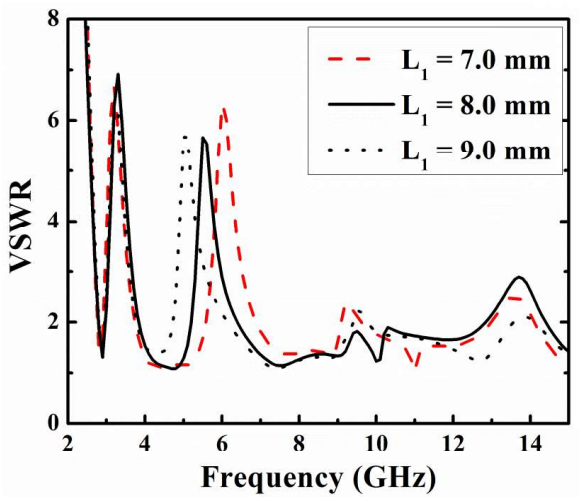


**Figure 4.7:** Simulated VSWR value of the antenna for variation in $L_1$

### 4.2.2 Results and Discussion

#### (a) VSWR Result

The optimized antenna prototype is fabricated and its characteristics are investigated. Figure 4.8 shows the top and bottom views of the fabricated prototype of the proposed UWB antenna. A vector network analyzer (VNA) E5071C is used for measurement. A good agreement is achieved between measured and simulated VSWR of the antenna as illustrated in Figure 4.9.The simulated results shows the operating bandwidth from 3-13.4 GHz with resonant frequencies at 3.1 GHz, 4.7 GHz, 7.5 GHz and 10 GHz. It is observed that the measured impedance bandwidth is from 3 GHz to 14 GHz, excluding rejection bands WiMAX/WLAN. However, some discrepancies are observed due to the measurement environment, SMA connector losses and the fabrication tolerances.

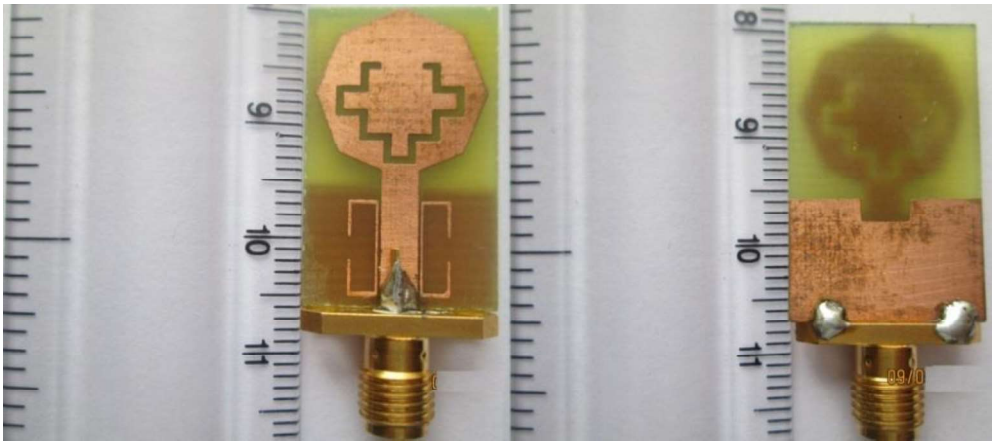

(a) (b)

**Figure 4.8:** Photograph of the fabricated antenna (a) Top View (b) Bottom view

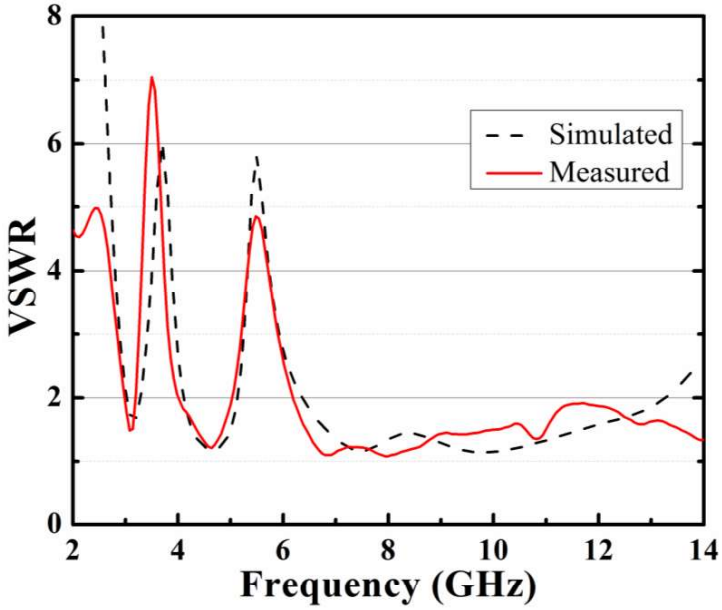


**Figure 4.9:** Comparison of the simulated and measured VSWR characteristics of the proposed antenna

**(b) Input Impedance Performance**

Simulated real and imaginary impedance of the antenna is shown in Figure 4.10. It is observed that at undesired WiMAX and WLAN band, a sharp decay in impedance is observed because of high VSWR accomplished in that region. In the rejection bands, the resistance part as well as reactance part shows a sharp decay. Therefore, it means the proposed antenna structure is opposing the wave propagation in that frequency region. The input reactance variation excluding notch bands is perceived between -30 to 30 Ω in the UWB range. This indicates the broadband nature of the proposed antenna. The positive and negative portion of reactance shows the inductive and capacitive nature of the structure. The real input impedance of the proposed antenna structure at resonant frequencies approaches to 50 Ω.

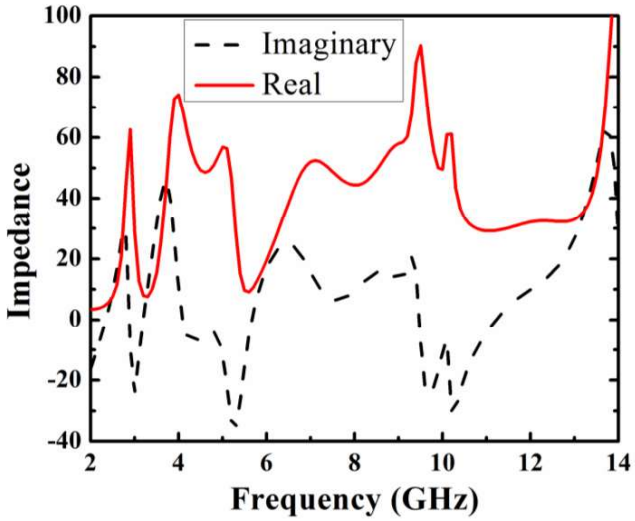


**Figure 4.10:** Simulated Impedance variation of the proposed antenna with frequency variation

**(c) Radiation Performance**

The radiation pattern including the co-polarization and cross-polarization of the proposed UWB antenna in the far field region is described using its principal E-plane (*xz*-plane) and H-plane (*yz*-plane) patterns for constant radial distance and frequency [Balanis, 2005] is displayed in Figure 4.11. It is observed that radiation pattern behavior is omnidirectional in H-plane and bidirectional pattern in E-plane. The measured gain of the antenna is presented in Figure 4.12 and gain variation within 3 dB range is achieved, except for notch band frequencies. The gain is significantly suppressed at notch frequencies, which clearly shows the effect of dual notch introduced in the geometry. The gain response shows steady response after 6 GHz.

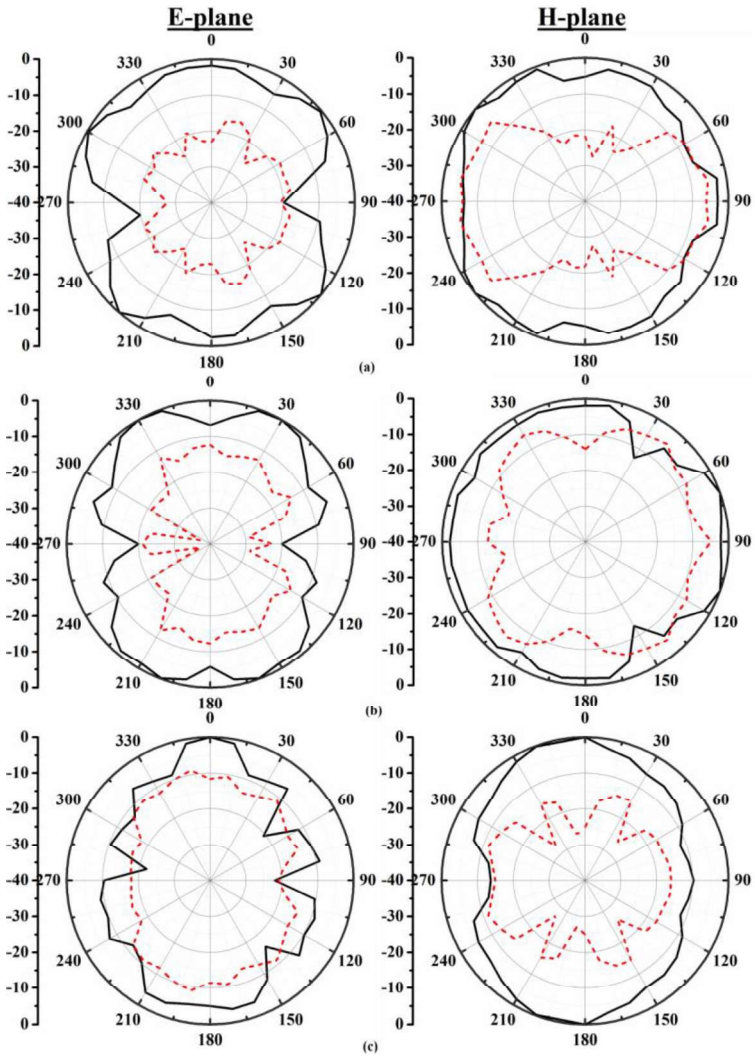


**Figure 4.11**: Measured radiation patterns with co polarization (—) and cross polarization (- - -) for H-planes and E-planes at (a) 4.7GHz (b) 7.5 GHz and (c) 10 GHz

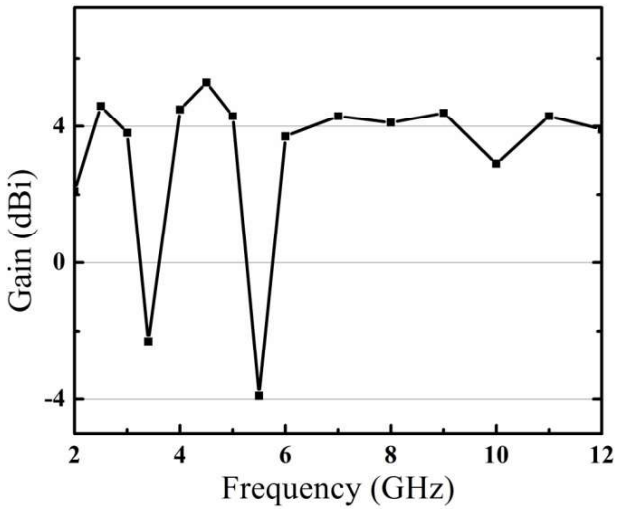


**Figure 4.12**: Measured gain of the proposed antenna

## 4.3 Hexagonal Shaped Koch Fractal UWB Antenna with Dual 3.5/5.5 GHz Band-notched Characteristics

### 4.3.1 Antenna Design

**(a) Antenna Configuration**

In this section, Koch geometry is applied at the edges of the hexagonal structure to utilize the space filling and multi-resonance phenomenon of the fractal geometry to achieve the miniaturization and wideband phenomena. The bandwidth enhancement is clearly observed due to the increment in electrical path length of the monopole because of fractal geometry application. In addition, dual C-shaped notches are inserted in the fractal monopole to get the band rejection in the WiMAX and WLAN operating bands. Figure 4.13 shows the optimized geometry of the proposed dual band notched fractal UWB antenna with dual band notch characteristics. In the evolution of presented antenna, hexagonal geometry works as an initiator, whereas Koch fractal works as a generator. The radiating monopole with feed line is printed on the top side of substrate, whereas ground structure is on other side. The proposed structure is simulated using HFSS v.13 on a rectangular substrate (W × L). Figure 4.14 shows the top and bottom view of the fabricated prototype on FR4 substrate, having a dielectric constant of $\varepsilon_r$ = 4.4, loss tangent tan δ = 0.023, and thickness of 1.6 mm. A rectangular substrate is taken initially for the proposed antenna because of its wideband operability and good radiation characteristics [Tasouji *et al.*, 2013; Cantrell, 2000]. The monopole is connected to a 50 Ω microstrip line of width ($W_m$) and length ($L_m$) for impedance matching. The ground plane is placed on the other side of the substrate having length ($L_g$) and width (W). The optimized parameters of the proposed fractal UWB antenna are: L = 31 mm, W = 27 mm, R = 8.9 mm, $L_g$ = 11.5 mm, $L_m$ = 12.2 mm, $W_m$ = 3.2 mm, $W_n$ = 0.5 mm, $C_1$ = 14 mm, $C_2$ = 5.2 mm, $C_3$ = 2 mm, $C_4$ = 9 mm, $C_5$ = 2 mm, and $C_6$ = 4 mm.

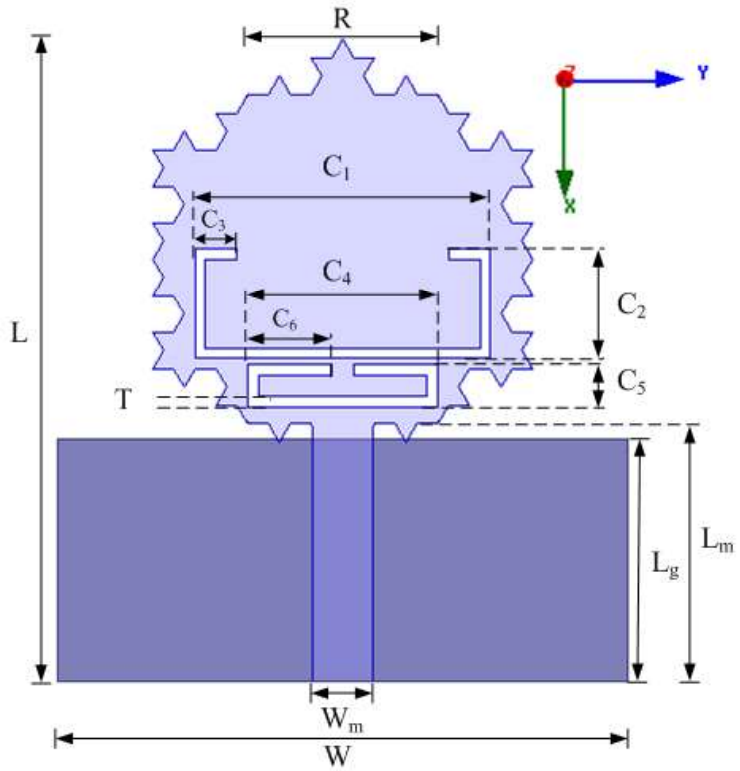


**Figure 4.13:** Geometry of the proposed dual notched fractal UWB antenna


**Figure 4.14:** Photograph of the fabricated antenna (a) top view and (b) bottom view

**(b) Effect of C-shaped slot**

To avoid the interference concerns in UWB operational band from WiMAX and WLAN band, a pair of C – shaped notch is introduced in the fractal UWB antenna. The length of the notch is approximately half wavelength at the center notch frequency and calculated using mathematical formula:

$$L_n = \frac{c}{2 f_n \sqrt{\frac{\varepsilon_r + 1}{2}}} \tag{4.5}$$

where $L_n$ is the length of the notch, $c$ is the speed of light, $\varepsilon_r$ is the dielectric constant, and $f_n$ is center notch frequency.

Therefore, two C-shaped notch are inserted in the monopole of the antenna. The notch frequency is decided by the dimensions of C-shaped notch. The surface current distribution at 3.5/5.5 GHz notch frequencies is shown in Figure 4.15(a) and (b). The current is mainly distributed around the interior and exterior edges of notch structure at notch frequencies. They are opposite in direction at each other. Therefore, radiation field is cancelled by each other and high attenuation is achieved at notch frequencies.

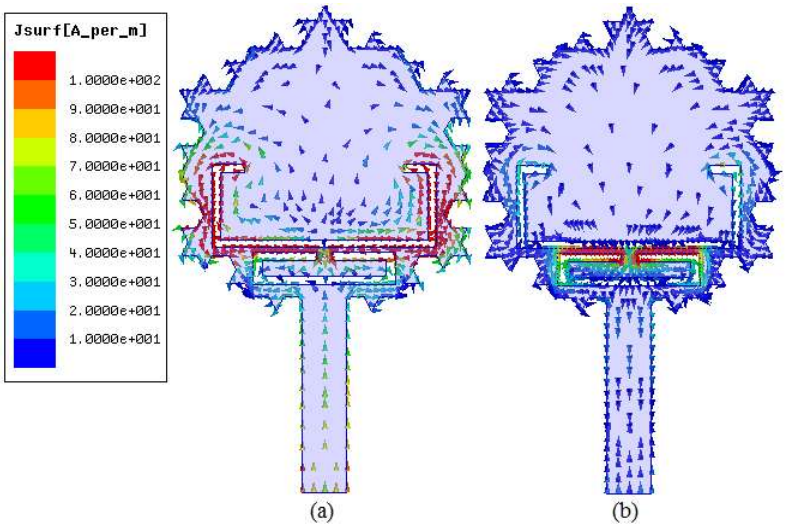


**Figure 4.15:** Simulated surface current distribution at (a) 3.5 GHz and (b) 5.5 GHz

**(c) Parametric Study**

The application of Koch geometry to achieve the desired characteristics is the effective part of the design. Moreover, parametric study of notch parameters is carried out to provide more insight behavior of the antenna. The width of notch is kept throughout $W_n$ = 0.5 mm, because of optimal response obtained for this thickness. The effect of dimension variation of $C_2$ on VSWR is shown in Figure 4.16. The variation in length from lower value to higher value decreases the VSWR level at notch frequency as well as distortion at higher frequencies too. Optimal response is obtained for $C_2$ = 5.0 mm. The effect of $C_3$ parameter variation from 1 to 3 mm on VSWR is shown in Figure 4.17. As the value of $C_3$ increases, VSWR value at 3.5 GHz notch frequency decreases, whereas for 5.5 GHz it shows shifting variations with VSWR changes.

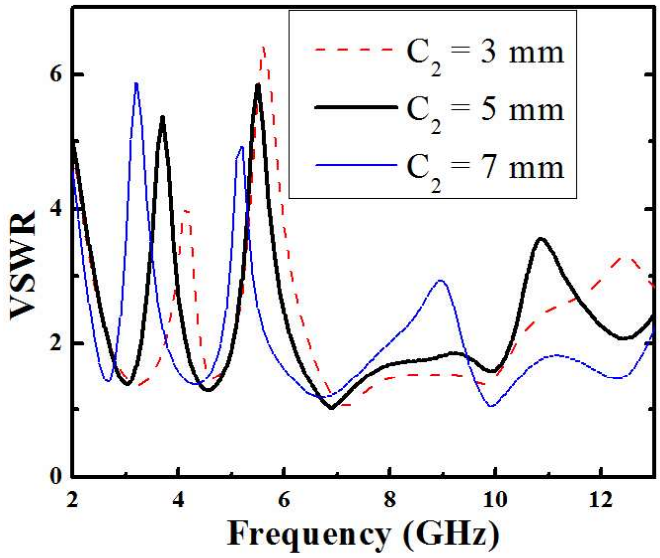


**Figure 4.16:** Simulated VSWR characteristic of the proposed fractal UWB antenna for different $C_2$

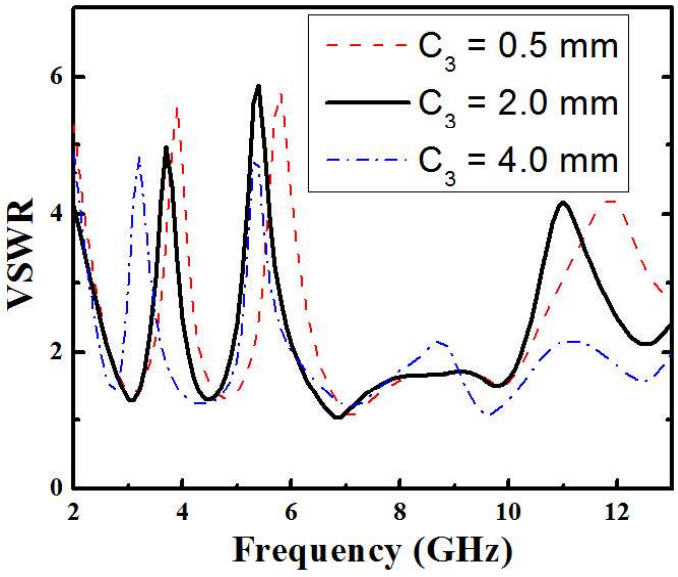


**Figure 4.17:** Simulated VSWR of the proposed fractal UWB antenna for different $C_3$

### 4.2.2 Results and Discussion

#### (a) VSWR Result

An Agilent vector network analyzer (VNA) E5071C is used to measure the VSWR. Figure 4.18 shows the simulated and measured VSWR of the proposed antenna. The measured VSWR shows wideband phenomena from 2.4 GHz to 11.7 GHz, excluding undesired dual notched bands. A good agreement is observed between simulated and measured results. However, some differences are observed due to SMA connector, soldering limitation and fabrication tolerances.

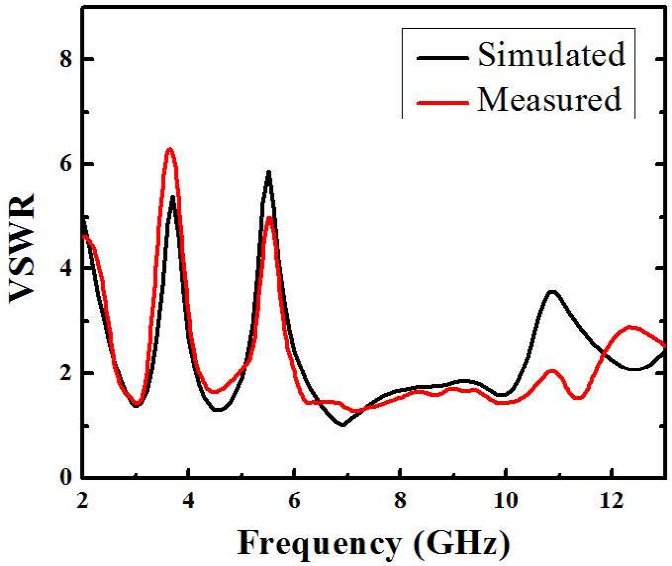


**Figure 4.18:** Measured and simulated VSWR of the proposed antenna

#### (b) Radiation Performance

The measured normalized radiation pattern in the H-plane (*yz*-plae) and E-plane (*xz*-plane) at resonant frequencies is shown in Figure 4.19. It is observed that H-plane pattern is nearly omnidirectional and E-plane is bidirectional as expected. The cross-polarization is increases with increase in frequencies. At higher frequency, the radiation pattern is distorted compared to lower resonant frequency because of change in current nature from standing wave nature at low frequencies to travelling wave nature at high frequencies. However, use of fractal geometry in antenna design helps to get the stable radiation pattern [Fereidoony *et al.*, 2012]. The measured gain of the fractal UWB antenna is shown in Figure 4.20. As expected, the measured gain decreases around 3.5 GHz and 5.5 GHz. Outside the notched band gain variation within 3 dBi is achieved. It indicates the stable gain characteristics by the proposed dual notched fractal UWB antenna.

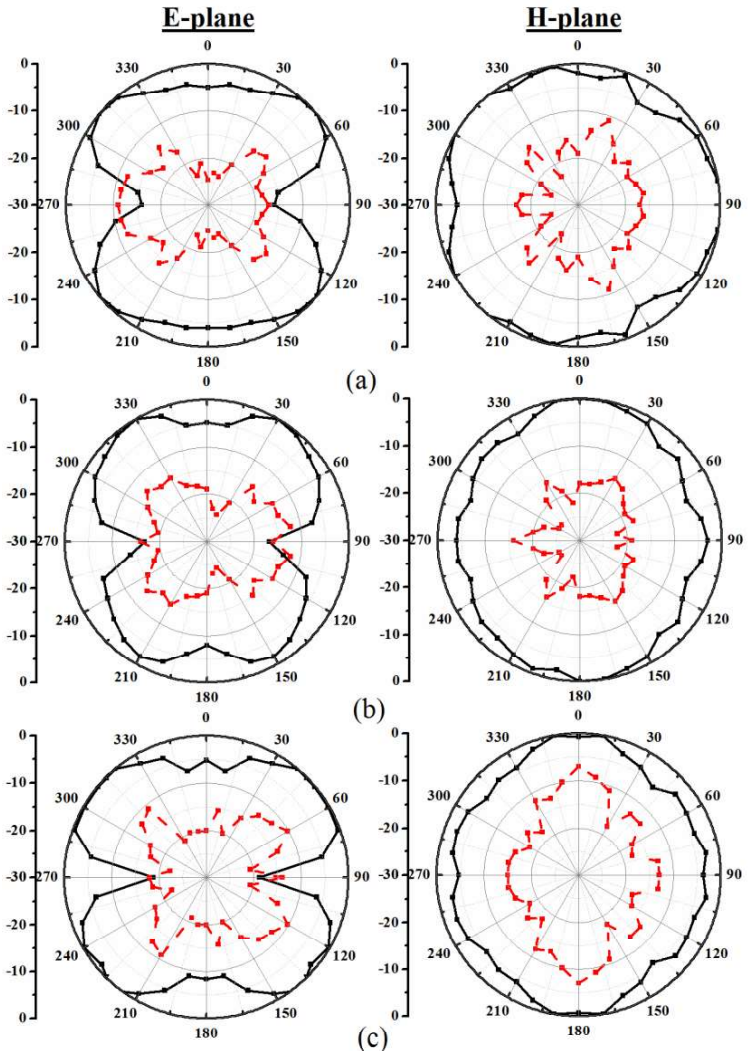


**Figure 4.19:** Measured radiation pattern with co-polarization (—) and cross-polarization (----) at resonant frequencies (a) 4.6 GHz, (b) 6.9 GHz, and (c) 9.9 GHz

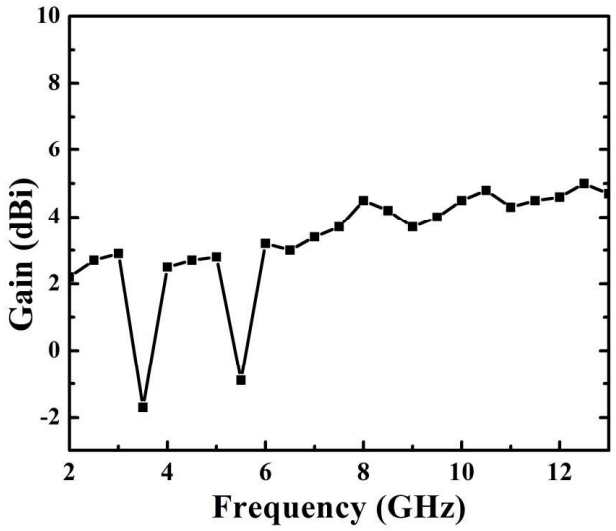


**Figure 4.20:** Measured gain of the proposed Antenna

**Table 4.2:** A Comparative analysis between proposed work and others available in the literature

| Antenna | Dimensions mm×mm×mm | Bandwidth (GHz) | Band-notch Band (GHz) |
|---|---|---|---|
| Work in Section 4.2 | 26×16.5×1.6 | 3-13.4 | 3.3-3.7, 5.15-5.825 |
| Work in Section 4.3 | 31×27×1.6 | 2.4-11.7 | 3.3-3.7, 5.15-5.825 |
| Abdollahvand *et al.*, 2010 | 20×18×1 | 2.8-11.8 | 3.3-3.7, 5.15-5.825 |
| Ojaroudi and Ojaroudi, 2013 | 18×12×0.8 | 2.7-12 | 3.3-3.7, 5.15-5.825 |
| Gao *et al.*, 2013 | 27×20×1 | 2.9-11.5 | 3.3-3.7, 5.15-5.825 |
| Azim *et al.*, 2014 | 14.5×14.75×1.6 | 3.1-11 | 3.3-3.7, 5.15-5.825 |

## 4.4 Summary

In this chapter, band rejection characteristics in the UWB band are studied. By introducing rectangular notch in the ground plane, impedance bandwidth behavior at higher frequency band gets improved. In order to achieve band reject characteristics, fractal slots as well as C-shaped slots are used in the antenna design. The applications of C-shaped slot provide narrowband rejection characteristics. In the first design, an octagonal shaped compact UWB antenna with dual band notch characteristics is presented. The etching of Minkowski fractal geometry based slot from the monopole provides the desired WiMAX rejection band, whereas placing of two C-shaped SSRRs on both the sides of the feed line provides band rejection at WLAN band. The proposed UWB antenna exhibits omnidirectional radiation pattern in H-plane and bidirectional radiation pattern in E-plane. The antenna gain varies from 2-5dBi, except at the notch bands. In case of second design, a compact fractal UWB antenna with dual band-notched characteristics has been presented and its characteristics are investigated. As we stated earlier, the application of fractal geometry provides desired miniaturization and wideband phenomena in UWB antenna design. The insertion of two C-shaped notches in monopole with proper dimensions helps to achieve band rejection in WLAN and WiMAX bands. The presented structure shows good VSWR response with stable radiation pattern. The antenna gain is decreases sharply at the notch bands. Moreover, a comparative study between proposed work in the chapter and the work presented in the literature is carried out, in the Table 4.2, in terms of antenna parameters such as dimension, operating bandwidth and notch-band. Hence, the presented structure can be a good choice for UWB applications. The compact size and good antenna characteristics of the presented antenna make it appropriate choice for UWB applications.

…